Nonlocal supercurrent of quartets in a three-terminal Josephson junction

Yonatan Cohen[a,1], Yuval Ronen[a,1], Jung-Hyun Kang[a], Moty Heiblum[a,2], Denis Feinberg[b], Régis Mélin[b], and Hadas Shtrikman[a]

[a]Department of Condensed Matter Physics, Braun Center for Submicron Research, Weizmann Institute of Science, 76100 Rehovot, Israel; and [b]Institut Néel, CNRS, Université Grenoble-Alpes, Institute of Engineering (INP), 38000 Grenoble, France

Edited by Eduardo Fradkin, University of Illinois at Urbana–Champaign, Urbana, IL, and approved May 21, 2018 (received for review January 2, 2018)

A novel nonlocal supercurrent, carried by quartets, each consisting of four electrons, is expected to appear in a voltage-biased three-terminal Josephson junction. This supercurrent results from a nonlocal Andreev bound state (ABS), formed among three superconducting terminals. While in a two-terminal Josephson junction the usual ABS, and thus the dc Josephson current, exists only in equilibrium, the ABS, which gives rise to the quartet supercurrent, persists in the nonlinear regime. In this work, we report such resonance in a highly coherent three-terminal Josephson junction made in an InAs nanowire in proximity to an aluminum superconductor. In addition to nonlocal conductance measurements, cross-correlation measurements of current fluctuations provided a distinctive signature of the quartet supercurrent. Multiple device geometries had been tested, allowing us to rule out competing mechanisms and to establish the underlying microscopic origin of this coherent nondissipative current.

nanowires | superconductivity | multiterminal JJ | quartet | nonlocal supercurrent

Superconductivity is an emblematical example of modern condensed matter physics as it manifests a macroscopic phenomenon governed by quantum mechanics, stressing the significance of the phase of a "macroscopic" wavefunction (1). Most striking is the dc Josephson effect (2). An established phase difference $\Delta\varphi$ between two superconductors (SCs) leads to a nondissipative supercurrent flow carried by Andreev bound states (ABS, Fig. 1). Biasing the two SCs junctions leads to time evolution of $\Delta\varphi$, resulting in an oscillatory supercurrent: the ac Josephson effect.

In recent years, multiterminal Josephson junctions (MTJs) have been considered as generalizations of the ubiquitous two-terminal junction (3–12). The MTJs are expected to show a wealth of new phenomena thanks to the existence of several independent phase variables. For instance, in equilibrium, dc supercurrent of Cooper pairs can flow from any terminal to another one, with the underlying ABS spectrum possessing topological features, such as robust zero-energy states (9–12). On the other hand, when biasing a three-terminal Josephson junction (3TJ), a new type of "multipair" dc supercurrent may emerge, involving all three terminals (3–6). The simplest multipair quasiparticles appear when $V_L = -V_R$, with both voltages applied to the S_L and S_R terminals, respectively, relative to the grounded terminal, S_M (Fig. 1*B*). Under this condition, two Cooper pairs, one emerging from S_L and one from S_R, are transferred to S_M through a quartet, which is composed of four electrons (3–6). As shown in Fig. 1*B*, this can happen only if $L < \xi$, with L the size of S_M and ξ is the superconducting coherence length. The quartet forms via "crossed-Andreev reflection" (CAR) (13–16). Evidently, the reversed process also takes place: two Cooper pairs in S_M split (each via a CAR process), and exchange electron partners that recombine to form two spatially separated Cooper pairs in terminals S_L and S_R. An ABS, involving four Andreev reflections within the 3TJ, is formed (Fig. 1*D*), carrying a nonlocal supercurrent where the current, say, from S_M to S_R, depends on the phase of S_L.

A previous study of the conductance in a diffusive metallic 3TJ already provided a signature of the quartet current (6); however, several alternative models for that current could not be ruled out. Here, we verify an emergent coherent quartet supercurrent in a 3TJ, which is formed in a proximitized semiconducting nanowire. Care was exercised to rule out other possible mechanisms such as multiple Andreev reflections (MAR) (7, 8, 17) and circuit electromagnetic coupling mechanisms (18, 19).

Quartet Supercurrent

The microscopic mechanism leading to the supercurrent in a short two-terminal superconductor–normal-superconductor Josephson junction (JJ) is described in Fig. 1*C*. An electron impinging on a superconductor with energy smaller than the single-particle superconducting energy gap may enter the superconductor as a Cooper pair while reflecting back a hole via Andreev reflection (AR). When two superconductors are placed in close proximity, an ABS forms, allowing a flow of an equilibrium supercurrent. The magnitude of the supercurrent obeys the energy-phase relation, $I = -(2e/\hbar)dE_{ABS}/d(\Delta\varphi)$, with E_{ABS} the energy of the ABS and $\Delta\varphi$ the phase difference between the two superconductors (20).

In a similar fashion the microscopic mechanism of the quartet supercurrent in a 3TJ is shown in Fig. 1*D*. Due to CAR processes in the small terminal S_M, an outgoing hole, in response to an incoming electron from one side, propagates toward the opposite terminal on the other side. A unique ABS is formed, with all three superconducting terminals participating via four ARs (3). At equilibrium ($V_L = V_R = 0$), the ABS energy $E_{ABS}(\varphi_L, \varphi_R)$ is a function of the two independent phases φ_L and φ_R, each with respect to that of the center terminal ($\varphi_M \equiv 0$). It is beneficial to choose new variables, $E_{ABS}(\varphi_q, \chi)$, where $\varphi_q = \varphi_L + \varphi_R$ and $\chi = \varphi_L - \varphi_R$. Under antisymmetric biasing conditions, $V = V_L = -V_R$ (Fig. 1*D*), using $\dot{\varphi}_{L,R} = (2e/\hbar)V_{L,R}$, the phase φ_q is stationary while the phase χ continuously changes, $\chi = (4e/\hbar)Vt$. In an

Significance

In this work we present detailed studies of a nondissipative current, called "quartet supercurrent," where two distinct Cooper pairs, originating in different terminals, recombine into a four-electron quasiparticle: a quartet. Employing conductance measurements and highly sensitive cross-correlation of current fluctuation, we identified the existence of such a coherent nonlocal state.

Author contributions: Y.C., Y.R., M.H., and H.S. designed research; Y.C., Y.R., J.-H.K., M.H., D.F., R.M., and H.S. performed research; Y.C., Y.R., M.H., D.F., and R.M. contributed new reagents/analytic tools; Y.C., Y.R., D.F., and R.M. analyzed data; and Y.C., Y.R., M.H., D.F., R.M., and H.S. wrote the paper.

The authors declare no conflict of interest.

This article is a PNAS Direct Submission.

[1]Y.C. and Y.R. contributed equally to this work.

[2]To whom correspondence should be addressed. Email: Moty.Heiblum@weizmann.ac.il.

This article contains supporting information online at www.pnas.org/lookup/suppl/doi:10.1073/pnas.1800044115/-/DCSupplemental.

Published online June 18, 2018.

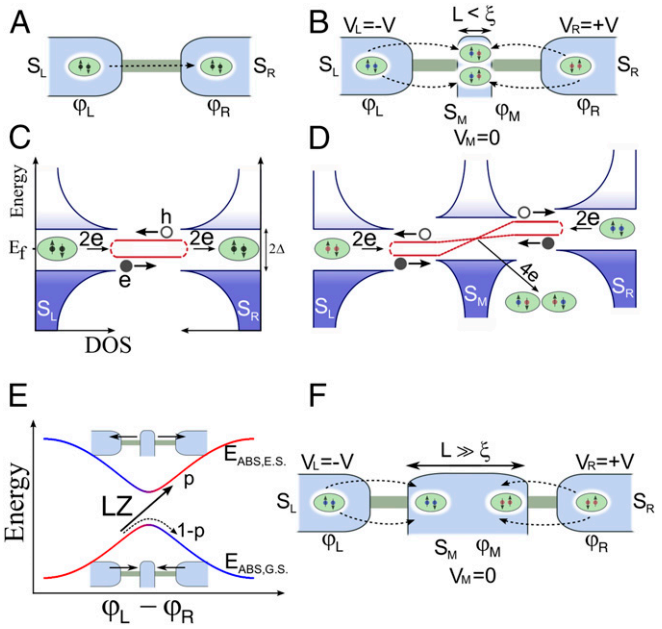

Fig. 1. Nondissipative current at 2- and 3TJs. (*A*) Schematic illustration of a two-terminal Josephson junction. (*B*) Schematic illustration of a 3TJ with a narrow central contact, and the formation of a quartet by combining two distinct Cooper pairs. (*C*) Schematic illustration of the two-terminal resonance process of an ABS, enabling Josephson supercurrent flow. (*D*) Schematic illustration of the three-terminal quartet ABS, leading to a nonlocal supercurrent flow. (*E*) Dependence of the two quartet particle–hole conjugates ABSs on the phase $\chi = \varphi_L - \varphi_R$. Evolution of the phase in time leads to Landau–Zener transitions, and thus fluctuations in the Josephson current. (*F*) Schematic illustration of a 3TJ with a wide central contact. Since the contact is much wider than the coherence length, Cooper pairs cannot form by electrons from opposite sides (CAR is suppressed) and thus quartets cannot form. Only single-pair ac Josephson current can flow between S_M and S_L, S_R.

adiabatic approximation at low bias, averaging the energy over the time evolution of χ, $\langle E_{ABS}(\varphi_q,\chi)\rangle_t$, yields a ϕ_q-dependent effective energy $E_{ABS,\mathit{eff}}(\varphi_q)$, with supercurrent $I_{\mathrm{quartet}} = -(4e/\hbar)dE_{ABS,\mathit{eff}}/d\varphi_q$. The charge $4e$ in the prefactor is the signature that current is carried by two Cooper pairs, namely, a quartet.

The nonlocal ABS depends on a single-phase φ_q, which drives the quartet current. However, possible quantum nonadiabatic (Landau–Zener) transitions between the lower and upper branches of the ABS add fluctuations to the dc quartet current (21, 22) (*SI Appendix*). Detailed calculations (4, 5, 8) show that the quartet current components in both branches $S_L - S_M$ and $S_R - S_M$ are equal even if the resistances of the two branches differ. This relates to their nondissipative, energy-conserving, processes. However, accompanying dissipative MAR processes of quasiparticles may not be equal in the two branches.

The existence of quartets relies on mediating CAR processes through the middle contact, S_M. Considering the geometry shown in Fig. 1*B*, the probability amplitude for a CAR process is expected to be large if $L < \xi_{Al} \sim 0.2 - 0.3\ \mu$m. Indeed, previous experiments have clearly shown the presence of a dominant CAR process in similar configurations based on InAs nanowires or on carbon nanotubes (13–16). This clearly applies to devices of the type d1 but not to devices of the type d2 (see below).

Quantum (nonequilibrium) noise is a powerful probe of quantum correlations in transport. A few comments on noise in Cooper pairs current are due. First, the equilibrium dc two-terminal Josephson current is, in principle, noiseless; namely, the ABSs support only fluctuations free dc current. However, thermal transitions between the two branches of the ABS, with each branch carrying an oppositely propagating current, evidently lead to current fluctuations (23, 24). Similarly, in a 3TJ device, the quartet current contains fluctuations (Fig. 1*E* and *SI Appendix*) (25). The fluctuations in both branches are expected to be positively correlated (25). Note that positive cross-correlations previously provided evidence for CAR in a normal-superconductor–normal Cooper splitting device (16).

Experimental Setup

Two different configurations of the three-terminal JJ were realized by coupling an aluminum superconducting contact to an InAs nanowire: device type d1—with the central contact S_M smaller than the superconductor coherence length (Fig. 2*A*); and device type d2—with the central contact S_M much larger than the superconductor coherence length (Fig. 2*B*).

The InAs nanowires were grown by the gold assisted molecular beam epitaxy process, using the well-established vapor–liquid–solid (VLS) growth technique. Growth was initiated on an unpatterned (100) InAs substrate, where single wires and Y-shaped intersections were simultaneously grown (26). The nanowires were spread on an oxidized P^+- doped Si wafer (with 150-nm-thick SiO_2), with superconducting contacts and local gates made by depositing 5-nm/120-nm Ti/Al on the wires. The setup allowed measuring the differential conductance and the "zero-frequency" cross-correlation (CC) of the current fluctuations in S_L and S_R (*SI Appendix*, section S2). We define the conductance $G_{L/R} = dI_{L/R}/dV_M$, where $I_{L/R}$ is

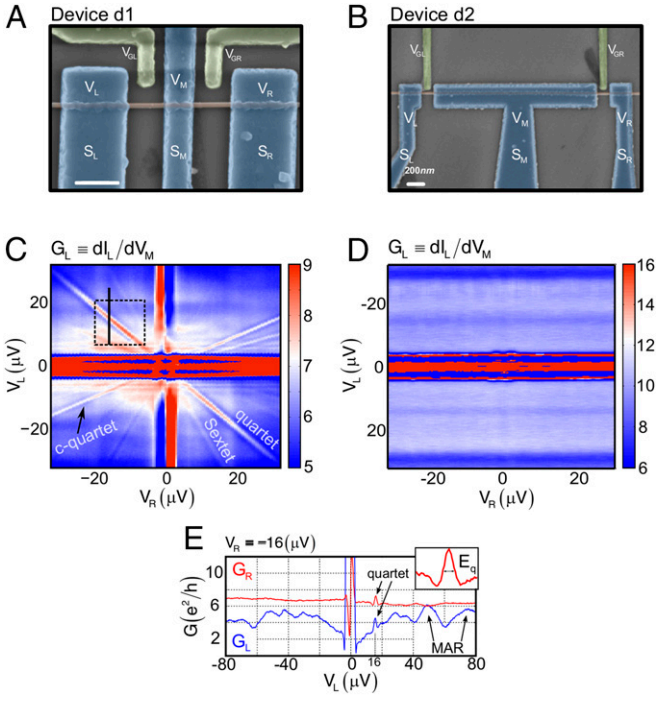

Fig. 2. Devices and differential conductance results. (*A*) SEM image of device d1. (Scale bar, 300 nm.) The central superconducting contact is 200 nm, namely, on the same order of magnitude as the coherence length. The gates (in green) were used to tune the transmission of the junction. (*B*) SEM image of device d2. (Scale bar is of length 300 nm.) The central superconducting contact is 3 μm wide, much larger than the coherence length. (*C*) G_L as a function of V_L and V_R measured in device d1. The quartet line, as well as other expected diagonal lines, is clearly seen. The solid line and dashed square are guidelines to Fig. 4*A*, Top and Fig. 4*B*. (*D*) G_L as function of V_L and V_R measured in device d2. No vertical or diagonal lines are observed. (*E*) G_L (blue) and G_R (red) as a function of V_L in d1. The shape of the quartet peak, which resembles the Josephson current with the two side dips, is shown in the upper right corner with the quartet energy.

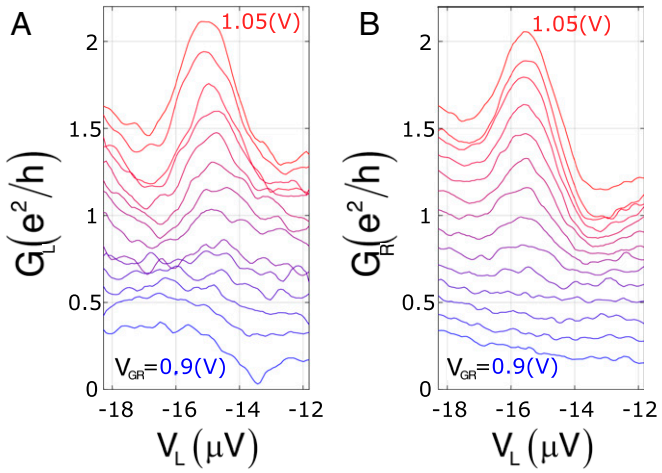

Fig. 3. Differential conductance correlation measurements between the right and left terminals. (*A* and *B*) G_L and G_R, respectively, as a function of the left contact bias V_L, and the right gate voltage V_{GR}, while V_R = 15 μV.

the current in S_L or S_R, and dV_M is a small ac signal applied to the central contact relative to ground. The dc bias was applied to S_L and S_R across two grounded 5Ω resistors.

The induced superconducting energy gap in the nanowire was found to be $2\Delta \approx 140$ μeV. The junctions were "short;" namely, some 200 nm long (between the SCs), with the conductance in the bias range of the MAR subgap states, with $G = (4-6)e^2/h$—far from the Coulomb blockade regime. For more information on the nanowires see refs. 26 and 27.

Results and Discussion

Differential Conductance Measurement. A color representation of G_L as a function of V_L and V_R in device type d1 is plotted in Fig. 2*C* (an equivalent plot of G_R is shown in *SI Appendix*, Fig. S2*B*). The equilibrium dc Josephson current is manifested as a wide "horizontal" structure ($V_L = 0$) in the "G_L plot." In the same plot the Josephson current in the right junction is observed as an attenuated "vertical" structure (being transconductance across the central contact). Similar results are obtained when plotting G_R.

Most importantly, a pronounced, Josephson-type, high-conductance peak is observed at $V_L = -V_R$, agreeing with the expected signature of the quartets. Other nondissipative processes are manifested by conductance peaks with different slopes, for example the "sextet" line at $V_R = -2V_L$ (and $V_L = -2V_R$), which represents a six-electron state (three Cooper pairs) (3–5, 8). In sharp contrast, the plot in Fig. 2*D*, representing the conductance in device type d2, has no sign of nonlocal effects, since CARs are not possible in the large S_M.

Fig. 2*E* shows traces of G_L and G_R as a function of V_L with $V_R = -16$ μV, with the sharp quartets conductance peaks appearing at $V_L = +16$ μV. Fig. 2*E* (*Inset*) shows a zoom into the quartet conductance peak in G_R, demonstrating the characteristic shape of a Josephson-like conductance peak, engulfed in two symmetric conductance dips (28, 29). The quartet supercurrent signature, which results from a coherent ABS, shared by all three terminals, is similar in both G_L and G_R, showing that a single microscopic mechanism takes place (Fig. 4*A*). In contrast, one can observe broader conductance peaks, appearing only in G_L. This results from MAR between S_L and S_M, with a width dictated by the interterminal transparencies and the quasiparticle density of states at the superconducting leads. The vertical displacement between G_L and G_R (Fig. 4*A*) is explained in *SI Appendix* using a simple resistively shunted junction model (*SI Appendix*, section S1*C*).

Tuning the transparency of each junction by the back-gate voltage, the differential conductance of S_L and S_R to ground is plotted in Fig. 3. The mutual correspondence between the left and right quartet currents is clearly demonstrated. Pinching the right-hand junction (with negative V_{GR}) quenches the quartet anomaly on both sides, hence confirming the observed correlation of quartet currents.

CC of Current Fluctuations: Experiment and Theory. To further verify the quartet anomaly we utilize a highly sensitive measurement of CC of current fluctuations in the left and right segments of 3TJ. In Fig. 4*A* we plot line-cuts of the differential conductance G_L and G_R as well as the corresponding CC as a function of V_L for $V_R = -15$ μV. A pronounced positive CC peak coincides with a peak in the differential conductance (Fig. 4*B*). This coincidence indicates that the current fluctuations in both sides of the device are positively correlated, as indicated by the currents anomaly, and thus cannot be a result of MAR processes. Moreover, the latter, involving fermionic quasiparticles dressed by Cooper pairs, would rather lead to a negative CC signal (30) (*SI Appendix*, section S1*D*). The evolution of the CC signal along the quartet conductance line, $V = V_L = -V_R$ (Fig. 4*C*, *Upper*), agrees qualitatively with numerical calculations based on nonequilibrium Green's functions (25) (*SI Appendix*). These calculations demonstrate that the quantum noise and the CC are both expected to be nonmonotonic with the voltage V, and thus reflect the nonadiabatic transitions between the two branches of the ABS (when a multiple of 2 eV matches the ABS spacing that varies with φ_q). Calculations also show that away from the resonance the typical quartet noise is on the order of $S_Q \approx e^2/h\Delta \sim 0.7 \cdot 10^{-27}\mathrm{A^2Hz^{-1}}$, in agreement with the experiment. We also extract from the measurement a critical quartet supercurrent of 0.6 nA. Note that the small negative fluctuating background in the CC signal (Fig. 4*A*) is ascribed to MAR processes (7, 8, 17, 31, 32).

Can an "Extrinsic" Effect Mimic the Quartet Current? An argument that relates the quartet conductance peak to an "extrinsic cause"

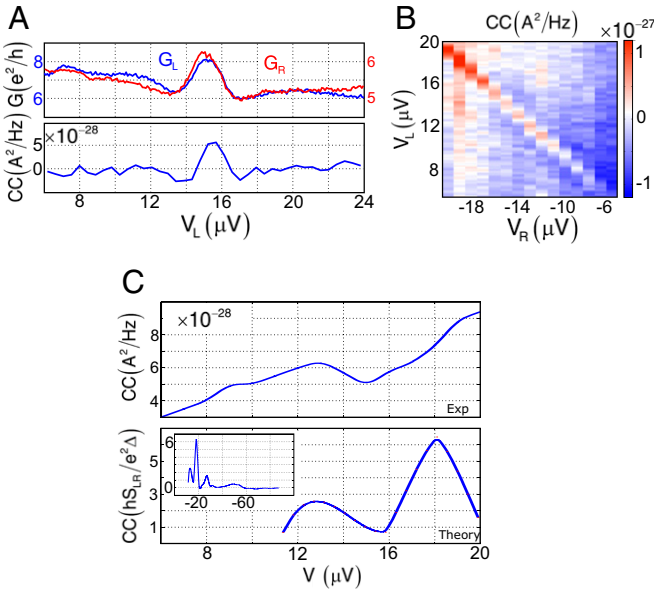

Fig. 4. CC of current fluctuations and nonlocal conductance measurements. (*A*, *Upper*) Differential conductance cuts of G_L and G_R along the solid line in Fig. 2*C*. (*A*, *Lower*) CC of current fluctuations at the left and right terminals. (*B*) CC as a function of V_L and V_R in the region defined by the dashed square of Fig. 2*C*. (*C*, *Upper*) CC along the quartet line. (*C*, *Lower*) Theoretical calculation of the CC (*SI Appendix*). The maxima are due to Landau–Zener resonances. (*Inset*) Zoom-out in the bias voltage range. It should be noted that the measured CC also drops beyond 20 μV.

should be addressed. Under quartet biasing condition, $V = V_L = -V_R$, the nanowire system is expected to generate two oscillating Josephson currents, with matching frequencies, $\dot{\varphi}_L = -\dot{\varphi}_R = 2$ eV$/\hbar$. Emitted radiation from one junction may resonantly be rectified by the other junction, leading to a dc signal. However, in the absence of an environment designed to be resonant at the Josephson frequency (as in ref. 33), this scenario (related to dynamical Coulomb blockade) requires a comparable circuit impedance with the quantum resistance. Moreover, in this scenario, the two types of devices, *d1* and d2, having similar electromagnetic environments (identical circuit coupling mechanisms), should have displayed the same anomalies, which they do not.

One may also argue that coupling between the two junctions is possible via the common resistance in the middle branch. This scenario was experimentally tested in coupled junctions at temperature close to *Tc* by Jillie et al. (18), and further discussed by Likharev (19). Testing the effect, a common resistance was performed by measuring the CC in the normal state. No CC signal was found, suggesting that the common resistance is much smaller than that of the individual junctions (*SI Appendix*).

Summary

We presented a detailed study of a nonlocal, coherent, Josephson current, under strong nonequilibrium conditions in a 3TJ. The dc nondissipative supercurrent was measured in an InAs nanowire in proximity to an aluminum superconductor. CAR processes led to a many-body quantum state, involving quartets, each composed of two Cooper pairs. Measurements of nonlocal conductance and CC of current fluctuations, performed on two types of 3TJ devices, provided a definite signature of the quartet supercurrent. Alternative mechanisms that may have produced similar effects are disproved. We provide theoretical support and estimates that agree qualitatively with the measured quantities.

ACKNOWLEDGMENTS. D.F. and R.M. acknowledge support from L'Agence Nationale de la Recherche Nanoquartets 12-BS-10-007-04 and the Centre Régional Informatique et d'Applications Numériques de Normandie computing center. M.H. acknowledges the partial support of the Israeli Science Foundation (ISF), the Minerva Foundation, and the European Research Council (ERC) under the European Community's Seventh Framework Program (FP7/2007-2013)/ERC Grant Agreement 339070. H.S. acknowledges partial support by ISF Grant 532/12, and Israel Ministry of Science and Technology (IMOST) Grants 0321-4801 and 3-8668. H.S. is incumbent of the Henry and Gertrude F. Rothschild Research Fellow Chair.

1. Bardeen J, Cooper LN, Schrieffer JR (1957) Theory of superconductivity. *Phys Rev* 108: 1175–1204.
2. Josephson BD (1962) Possible new effects in superconductive tunneling. *Phys Lett* 1: 251–253.
3. Freyn A, Douçot B, Feinberg D, Mélin R (2011) Production of nonlocal quartets and phase-sensitive entanglement in a superconducting beam splitter. *Phys Rev Lett* 106: 257005.
4. Cuevas JC, Pothier H (2007) Voltage-induced Shapiro steps in a superconducting multiterminal structure. *Phys Rev B* 75:174513.
5. Jonckheere T, et al. (2013) Multipair Josephson resonances in a biased all-superconducting bijunction. *Phys Rev B* 87:214501.
6. Pfeffer AH, et al. (2014) Subgap structure in the conductance of a three-terminal Josephson junction. *Phys Rev B* 90:075401.
7. Houzet M, Samuelsson P (2010) Multiple Andreev reflections in hybrid multiterminal junctions. *Phys Rev B* 82:060517.
8. Mélin R, Feinberg D, Douçot B (2016) Partially resumed perturbation theory for multiple Andreev reflections in a short three-terminal Josephson junction. *Eur Phys J B* 89:67.
9. van Heck B, Mi S, Akhmerov AR (2014) Single fermion manipulation via superconducting phase differences in multi-terminal Josephson junctions. *Phys Rev B* 90: 155450.
10. Riwar R-P, Houzet M, Meyer JS, Nazarov YV (2016) Multi-terminal Josephson junctions as topological matter. *Nat Commun* 7:11167.
11. Strambini E, et al. (2016) The ω-SQUIPT as a tool to phase-engineer Josephson topological materials. *Nat Nanotechnol* 11:1055–1059.
12. Padurariu C, et al. (2015) Closing the proximity gap in a metallic Josephson junction between three superconductors. *Phys Rev B* 92:205409.
13. Hofstetter L, Csonka S, Nygård J, Schönenberger C (2009) Cooper pair splitter realized in a two-quantum-dot Y-junction. *Nature* 461:960–963.
14. Herrmann LG, et al. (2010) Carbon nanotubes as cooper-pair beam splitters. *Phys Rev Lett* 104:026801.
15. Hofstetter L, et al. (2011) Finite-bias Cooper pair splitting. *Phys Rev Lett* 107:136801.
16. Das A, et al. (2012) High-efficiency Cooper pair splitting demonstrated by two-particle conductance resonance and positive noise cross-correlation. *Nat Commun* 3:1165.
17. Octavio M, Tinkham M, Blonder GE, Klapwijk TM (1983) Subharmonic energy-gap structure in superconducting constrictions. *Phys Rev B* 27:6739–6746.
18. Jillie DW, Nerenberg MAH, Blackburn JA (1980) Voltage locking and other interactions in coupled superconducting weak links. *Phys Rev B* 21:125–131.
19. Likharev K (1986) *Dynamics of Josephson Junctions and Circuits* (Gordon and Breach, New York).
20. Kulik IO (1970) Macroscopic quantization and proximity effect in S-N-S junctions. *Sov Phys JETP* 30:944.
21. Goffman MF, et al. (2000) Supercurrent in atomic point contacts and andreev states. *Phys Rev Lett* 85:170–173.
22. Bergeret FS, Virtanen P, Heikkilä TT, Cuevas JC (2010) Theory of microwave-assisted supercurrent in quantum point contacts. *Phys Rev Lett* 105:117001.
23. Martín-Rodero A, Levy Yeyati A, García-Vidal FJ (1996) Thermal noise in superconducting quantum point contacts. *Phys Rev B Condens Matter* 53:R8891–R8894.
24. Averin D, Imam HT (1996) Supercurrent noise in quantum point contacts. *Phys Rev Lett* 76:3814–3817.
25. Mélin R, Sotto M, Feinberg D, Caputo J-G, Douçot B (2016) Gate-tunable zero-frequency current cross correlations of the quartet state in a voltage-biased three-terminal Josephson junction. *Phys Rev B* 93:115436.
26. Kang J-H, et al. (2013) Crystal structure and transport in merged InAs nanowires MBE grown on (001) InAs. *Nano Lett* 13:5190–5196.
27. Ronen Y, et al. (2016) Charge of a quasiparticle in a superconductor. *Proc Natl Acad Sci USA* 113:1743–1748.
28. Barone A, Paternó G (1982) *Physics and Applications of the Josephson Effect* (Wiley, New York).
29. Ambegaokar A, Halperin B (1969) Voltage due to thermal noise in the dc Josephson effect. *Phys Rev Lett* 22:1364–1366.
30. Duhot S, Lefloch F, Houzet M (2009) Cross correlation of incoherent multiple Andreev reflections. *Phys Rev Lett* 102:086804.
31. Cuevas JC, Martín-Rodero A, Levy Yeyati A (1999) Shot noise and coherent multiple charge transfer in superconducting quantum point contacts. *Phys Rev Lett* 82: 4086–4089.
32. Cron R, Goffman MF, Esteve D, Urbina C (2001) Multiple-charge-quanta shot noise in superconducting atomic contacts. *Phys Rev Lett* 86:4104–4107.
33. Hofheinz M, et al. (2011) Bright side of the Coulomb blockade. *Phys Rev Lett* 106: 217005.